The Heparin−Ca^{2+} Interaction: Structure of the Ca^{2+} Binding Site

Franck Chevalier,[a] Jesús Angulo,[a] Ricardo Lucas,[a] Pedro M. Nieto,*[a] and Manuel Martín-Lomas[a]

Dedicated to Prof. Julio D. Martín on the occasion of 60th birthday

Keywords: Calcium / Carbohydrates / Heparin / Molecular modelling / NMR spectroscopy

Heparin as a polyelectrolyte may exhibit cation-territorial or site-specific binding, depending on the counterion. Thus, while Ca^{2+} binds specifically, Na^+ or Mg^{2+} do so territorially. We have explored the utility of computational methods that combine the calculation of the interaction energy potential with molecular dynamics simulation for the study of the cation interaction with **1**. The computational procedure was designed in order to provide an accurate calculation of the interaction energy and to account simultaneously for the flexibility of the charged heparin side chains. This procedure was able to reproduce the behaviour of Na^+, Ca^{2+}, and Mg^{2+}, suggesting that it was the combination of charge and size in Ca^{2+} that was responsible for its site-specific binding. Other known characteristics of this interaction were also reproduced, as was the displacement of the iduronate conformational equilibrium. The interaction potential results allowed the Ca^{2+} binding site between consecutive glucosamine and iduronate residues to be identified. A model disaccharide **2** was synthesised and its behaviour in the presence of Ca^{2+} was studied by NMR spectroscopy, confirming the location of the cation binding site within the glucosamine–iduronate disaccharide.

Introduction

Heparin and heparan sulfate are sulfated glycosaminoglycans (GAGs)[1,2] basically constituted of disaccharide repeating units of L-iduronic acid and D-glucosamine linked by α-1→4-glycosidic linkages and typically containing sulfate groups at positions 2 of the L-iduronic acid units and 2 and 6 of the D-glucosamine units. Heparin and heparan sulfate interact with a number of extracellular proteins, modulating their activity.[1−5] These include the fibroblast growth factors (FGFs), a family of signalling proteins that activate a membrane receptor (fibroblast growth factor receptor or FGFR) by interacting with heparin and promote intracellular signalling.[3−5] Several of these heparin or heparan sulfate protein interactions involve cations.[6,7] Both heparin and heparan sulfate are ionic polysaccharides with specific physicochemical properties, due to their polyelectrolyte nature.[8] It has been proposed that counterions bind to polyelectrolytes either territorially or site-specifically. Territorial binding involves long-range electrostatic interactions with the solvated counterion, which becomes delocalised within a certain volume around the polyion. Site-specific binding implies replacement of the counterion solvent coordination shell by the charged groups of the polyion, yielding a spatially defined complex.[8] ^1H chemical shift, ^{23}Na relaxation, and NOE NMR spectroscopic data have shown that Na^+, Ca^{2+}, and Mg^{2+} interact with the low-pH carboxylic form of heparin through delocalised, long-range electrostatic interactions. At higher pH values, however, Na^+ and Mg^{2+} continue to interact in the same manner, but there is a site-specific contribution to the binding of Ca^{2+}.[9] These observations can be interpreted in terms of the existence of specific calcium binding sites in the structure of these GAGs.

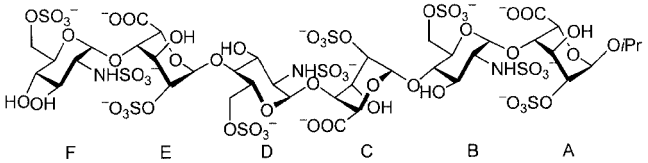

1

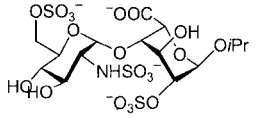

2

Because of its physiological relevance, we have previously investigated the interaction between Ca^{2+} and heparin with the aid of the model synthetic hexasaccharide **1**.[10] We observed that the presence of Ca^{2+} caused significant changes

[a] Grupo de Carbohidratos, Instituto de Investigaciones Químicas, CSIC,
Isla de la Cartuja, Américo Vespucio s/n, 41092 Seville, Spain
Fax: (internat.) + 34-95/446-0565
E-mail: Pedro.Nieto@iiq.cartuja.csic.es

in some signals of the ^{1}H NMR spectrum of **1**, thus suggesting some selectivity in the Ca^{2+}−hexasaccharide **1** interaction. The behaviour of **1** and Ca^{2+} was explored by molecular dynamics, and these calculations predicted that some regions of the surface of **1** should interact specifically with Ca^{2+} but not with Na^+. On this basis we proposed three possible heparin Ca^{2+}-binding sites, arranged within a network of sulfate and carboxylate groups.[10] We have extended these investigations and now report a quantitative method based on the calculation of the cation interaction potential for study of the cation−**1** interaction.[11,12] By this method we have been able to improve the definition of the main heparin calcium-binding site. Additionally, and in order to provide additional experimental support for the theoretical predictions, we have synthesised the disaccharide GlcN-IdoA **2**, containing just one of the three Ca^{2+}-binding sites proposed for **1** and incapable of displaying polyionic properties, due to its reduced size. The effects of the presence of Ca^{2+} on **2** were monitored by NMR, and the cation interaction was modelled and compared with that of **1**. The changes in coupling constants observed upon addition of Ca^{2+} indicated that the disaccharide had an appreciable affinity for this cation, detectable as a consequence of an induced conformational change in the iduronate ring.

Results and Discussion

The main interactions between heparin and ions are electrostatic in nature and take place through the charged saccharide groups. These groups are located mainly on flexible side chains, and the local shape of the surface therefore changes dramatically with the orientation of these groups. The plasticity of this system should therefore be carefully considered. Bearing this problem in mind, we have previously used molecular dynamics as a "flexible" docking technique that allowed the side chain conformational space of **1** to be explored and its interaction with cations to be evaluated.[10] This approach, in spite of its simplifications, was able to predict a stronger interaction for Ca^{2+} than for Na^+ and to support experimental NMR spectroscopic data such as chemical shift and line shape.[10] These results prompted us to propose a preferred Ca^{2+} binding site and two secondary binding sites.[10] This method, however, implied the evaluation of the binding sites in terms of occupancy along a MD trajectory, and it was difficult to quantify the strength of the interaction for comparisons. Furthermore, it needed a careful adjustment of the dielectric constant. We have now explored the utility of rigid body docking methods, as implemented in the program GRID,[11] to deal with this problem. Since these methods do not consider the full flexibility of the partners, we used an ensemble of structures obtained from MD simulations, which should take account of the system flexibility.

The influence of the side chain conformation of **1** on the interactions with Ca^{2+} and Na^+ was explored first. The representative ensemble used was composed of 32 structures, which were constructed by combination of all the possible values for significant torsion angles found in **1**. The choice of these critical angles and their values was based on current knowledge of the heparin structure as well as on our previous structural study of **1**.[1,13,14] It is well established that iduronate residues in heparin exist in a conformational equilibrium between a chair $^1C_4$ and a skew-boat ^2S_O form.[10] Both $^1C_4$ and ^2S_O iduronate conformers were thus considered. On the other hand, the adiabatic energy maps of the glycosidic linkages between IdoA and GlcN residues showed two subminima that were also predicted by molecular dynamics simulations,[13,15] and so four more possible conformers were also considered. The GlcN ω rotamer was fixed to *gg*, as we had previously determined, on the basis of coupling constants and NOEs, that this was the more populated rotamer for **1**.[10,13] The rest of the torsion angles that might influence the arrangement of the charged groups were analysed by molecular dynamics.[13] Since the torsion angles of the GlcN 6-*O*-sulfate groups changed significantly in MD simulation, two different orientations were also considered for them. The values of the angles defining the IdoA-GlcN glycosidic linkages and the orientations of GlcN 6-*O*-sulfate groups (see Figure 1) were both taken from the more frequently visited torsion angles in a previous MD simulation in the absence of counterions.[13]

The results were first analysed in terms of the most favourable interaction energy with Ca^{2+} (Table 1), and it was conclusively shown that GRID correctly predicted a higher affinity of Ca^{2+} for the iduronate $^1C_4$ conformer than for the iduronate ^2S_O one. This is a well-known Ca^{2+}-binding effect on the iduronate conformational equilibrium assessed by NMR.[14] Regarding the influence of the glycosidic and side-chain torsion angles, the higher interaction energy conformers had the same value of the χ_4 angle (Table 1, Entries 1, 5, 25, 29). This group of four conformers also had the highest energy for the interaction with Na^+. We interpreted this observation as an indication of the importance of the flexibility of the sulfate side chains on the interaction.

The interaction of **1** with Na^+ was then studied in order to examine the NMR evidence mentioned above[9] regarding the different binding of this counterion as compared with Ca^{2+}. The interaction with Na^+ was extensively screened by the same ensemble as for Ca^{2+} (Table 1). Although the conformers with higher interaction energies had the same geometries as with Ca^{2+}, the differences in interaction energy between them and the rest of the structures were smaller than those found for Ca^{2+} (Table 1). The standard deviations of the interaction energies of the conformers under consideration were 8.5 for Ca^{2+} and 4.7 kcal·mol^{-1} for Na^+. This smaller dispersion of the interaction energies within the ensemble with Na^+ was interpretable as a consequence of better organization of the binding site for Ca^{2+} than for Na^+. Thus, Ca^{2+} achieved additional stabilization due to a better complementarity, while the behaviour of Na^+ may reflect an unspecific electrostatic interaction.

Experimental evidence has shown that Mg^{2+}, similarly to Na^+ and unlike Ca^{2+}, is territorially bound to heparin.[9]

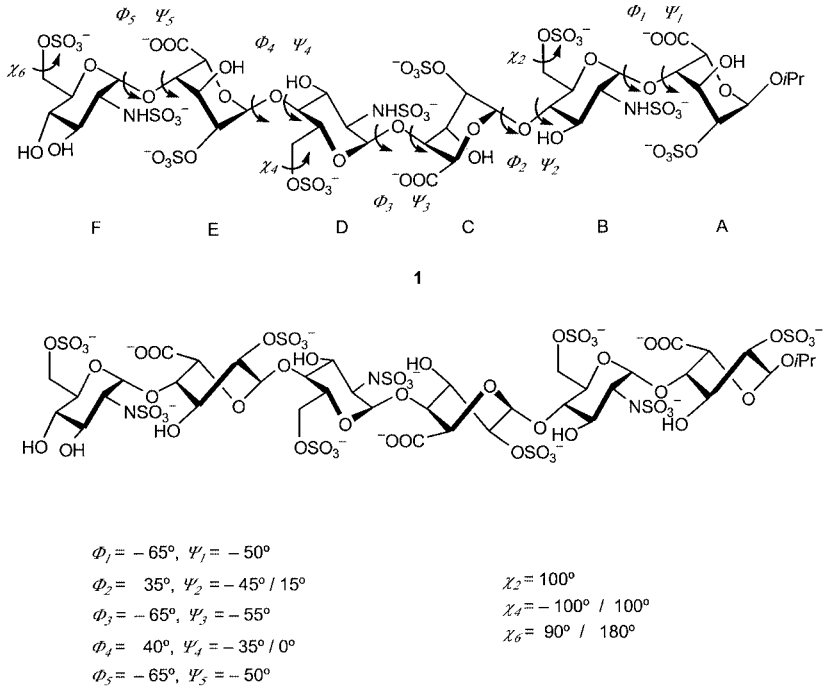

Figure 1. Torsion angles considered for the construction of the ensemble of structures used in the calculation of the cation interaction energy and the values used

This observation suggested that the combination of cation charge and size was responsible for the site-specific binding to heparin. The interaction potentials for Na^+, Ca^{2+}, and Mg^{2+} were thus calculated in order to study this feature. The calculations were carried out with only one model of **1** for each of the $^1C_4$ and ^2S_o conformers. These models were constructed by relaxation in the presence of the corresponding cation, using as the starting geometry that corresponding with the best interacting conformers of **1** (Table 1, Entry 5 for $^1C_4$ conformer and Entry 6 for ^2S_o conformer). The more favourable interaction energies for the $^1C_4$ and ^2S_o forms are given in Table 2. The interaction energies were more favourable for Ca^{2+} than for either Na^+ or Mg^{2+}, according to the experimental evidence.[9] All three cations showed a preference for the $^1C_4$ form, but this was larger for Ca^{2+} than for Na^+ or Mg^{2+}. It is worth noting that these results indicated that Mg^{2+} was more similar to Na^+ than to Ca^{2+} in spite of its charge. This agreed with those experimental data that had been interpreted in terms of a territorial type of binding for Na^+ and Mg^{2+} and a site-specific binding for Ca^{2+}.[9]

Finally, the topologies of the regions displaying better interactions with Ca^{2+} were analysed. The topology resembled that proposed on the basis of molecular dynamics and NMR spectroscopic data for hexasaccharide **1** (Figure 2).[10] The main sites for all three cations studied were located between consecutive $GlcN_{i+1}$−$IdoA_i$ residues and involved the 5-COO^- and 2-OSO_3^- groups of iduronate and the 2-$NHSO_3^-$ of glucosamine. The specificity of the interaction was also evaluated by computing the volume of the region of stronger interaction energy within an energy window of 25 kcal·mol^{-1} from the lowest interaction energy (Table 2).[12] Although the favourable interaction regions were similar, the volume for Ca^{2+} was smaller than those for Na^+ or Mg^{2+}, which again were similar to each other (Figure 3, Table 2). These results, like the dispersions of energy values among the conformers, pointed to stricter geometrical requirements and higher specificity for Ca^{2+} binding than for that of Na^+ or Mg^{2+}. This finding reproduced the previous result from MD, in which, in a mixed experiment, Ca^{2+} ions were more localised than Na^+ along the trajectory in this type of site (Figure 2).[10]

In summary, the calculations predicted that Ca^{2+}, in comparison with Na^+ and Mg^{2+}, would have the highest interaction energy with hexasaccharide **1**, located in the smallest volume, and would be more sensitive to conformational changes. These observations were in agreement with a defined Ca^{2+}-binding site suitable for both its charge and volume.

In an attempt to gain additional experimental support for the predictions from the above calculations, we synthesised disaccharide **2** and investigated its Ca^{2+}-binding properties by NMR spectroscopy. Disaccharide **2** contained the minimum structural requirements for the main site-specific binding previously proposed by us.[10] The synthesis of **2** was carried out from 6-*O*-acetyl-2-azido-2,6-di-*O*-benzyl-2-deoxy-D-glucopyranosyl trichloroacetimidate (**3**) and methyl-3-*O*-benzyl-1-*O*-dimethylthexylsilyl-β-L-idopyranuronate (**4**), as indicated in Scheme 1. Glycosylation of **4** with **3** took place regio- and stereoselectively[13] to give the corresponding α1→4-linked disaccharide, which after conventional benzoylation afforded compound **5** (70%, two steps). The anomeric position of **1** was deprotected (85%) and activated as the corresponding trichloroacetimidate **7**

Table 1. Maximum interaction energies [kcal·mol^{-1}] calculated by GRID for **1** conformers; some of the considered conformers has severe steric interactions and were disregarded

	Interaction energy [kcal mol^{-1}]			Conformer [°]			
Entry	Ca^{2+}	Na^{+}	Iduronate	Ψ_2	Ψ_4	χ_6	χ_4
1	−86	−46	$^1C_4$	−35	−45	180	−100
2	−83	−45	^2S_O	−35	−45	180	−100
3	−76	−40	$^1C_4$	−35	−45	180	100
4	−68	−37	^2S_O	−35	−45	180	100
5	−87	−47	$^1C_4$	−35	−45	90	−100
6	−84	−46	^2S_O	−35	−45	90	−100
7	−76	−41	$^1C_4$	−35	−45	90	100
8	−68	−37	^2S_O	−35	−45	90	100
9	–	–	$^1C_4$	0	15	180	−100
10	−77	−42	^2S_O	0	15	180	−100
11	−75	−41	$^1C_4$	0	15	180	100
12	−68	−37	^2S_O	0	15	180	100
13	–	–	$^1C_4$	0	15	90	−100
14	–	–	^2S_O	0	15	90	−100
15	−76	−41	$^1C_4$	0	15	90	100
16	−68	−37	^2S_O	0	15	90	100
17	–	–	$^1C_4$	−35	−45	180	−100
18	–	–	^2S_O	−35	−45	180	−100
19	−75	−41	$^1C_4$	−35	−45	180	100
20	−68	−37	^2S_O	−35	−45	180	100
21	–	–	$^1C_4$	−35	−45	90	−100
22	–	–	^2S_O	−35	−45	90	−100
23	−76	−41	$^1C_4$	−35	−45	90	100
24	−68	−37	^2S_O	−35	−45	90	100
25	−85	−46	$^1C_4$	0	15	180	−100
26	−83	−45	^2S_O	0	15	180	−100
27	−77	−41	$^1C_4$	0	15	180	100
28	−68	−37	^2S_O	0	15	180	100
29	−86	−46	$^1C_4$	0	15	90	−100
30	−84	−46	^2S_O	0	15	90	−100
31	−77	−41	$^1C_4$	0	15	90	100
32	−68	−37	^2S_O	0	15	90	100

Table 2. Most favourable interaction energies calculated for minimised **1** with all iduronate residues in the $^1C_4$ and ^2S_O conformations, in kcal·mol^{-1}; the volumes of the regions with the highest interaction energies, up to 25 kcal·mol^{-1} above the optimum, are given between brackets as percentages of the total volume considered around the hexasaccharide

Metal cation	$^1C_4$	^2S_o
Ca^{2+}	−95 (4)	−80 (4)
Na^{+}	−52 (23)	−43 (76)
Mg^{2+}	−50 (32)	−45 (57)

(90%). The isopropyl glycoside **8** was then prepared (60%) by treatment of **7** with isopropyl alcohol. Debenzoylation of **8**, followed by *O*-sulfation, afforded **10**, which was catalytically hydrogenated and *N*-sulfated to yield **2** (80%). The interactions between **2** and the counterions were first investigated by use of the calculation approach described above. Two models, with the iduronate ring in the $^1C_4$ and in the ^2S_O conformations, respectively, were constructed with the geometries that had given the optimum energy values in the case of **1**, and were further relaxed. The calculated most

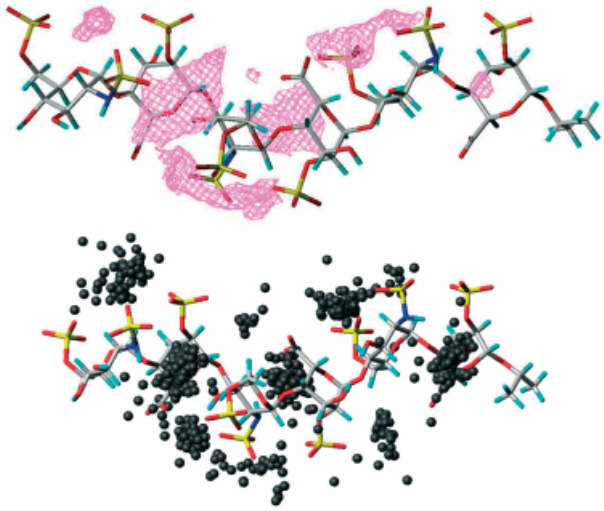

Figure 2. Most favourable Ca^{2+} interaction regions in **1** (25 kcal mol^{-1} above the minimum) (top) and positions of calcium cations along a 9 ns MD trajectory (bottom)[10]

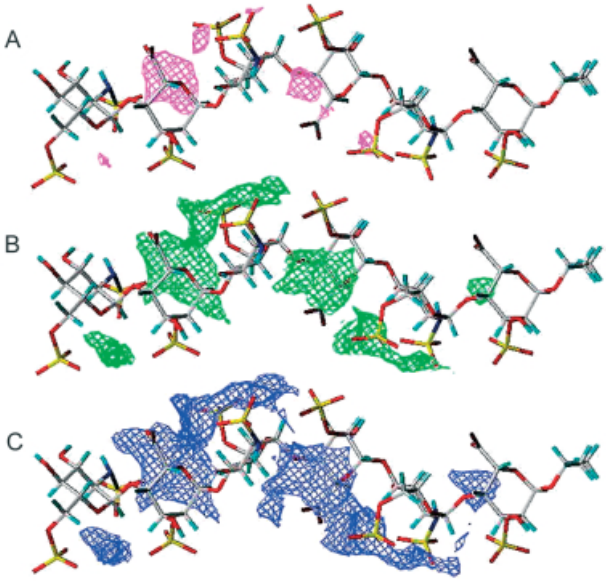

Figure 3. Structure of hexasaccharide **1** used for the calculation of the cation interaction energy and the volumes of the regions of the interaction potential within 15 kcal·mol^{-1} above the lowest values for: a) Ca^{2+}, b) Na^{+}, and c) Mg^{2+}

favourable interaction energies with Ca^{2+}, Na^{+}, and Mg^{2+} are given in Table 3. Trends similar to those seen for **1** were observed, Ca^{2+} showing the strongest interaction energy. Secondly, the more favourable region was located between the glucosamine and iduronate residues, the same charged groups were involved in the interaction, and the interaction volumes were smaller for Ca^{2+} than for Na^{+} (Figure 4). The $^1C_4$ conformer again showed the highest cation affinity. Comparison between the better results of **1** and **2** indicated that calcium interacted more strongly with the hexasaccharide. This could be explained in terms of the contribution of medium- and long-range electrostatics present in the case of **1**, which may stabilise the complex.

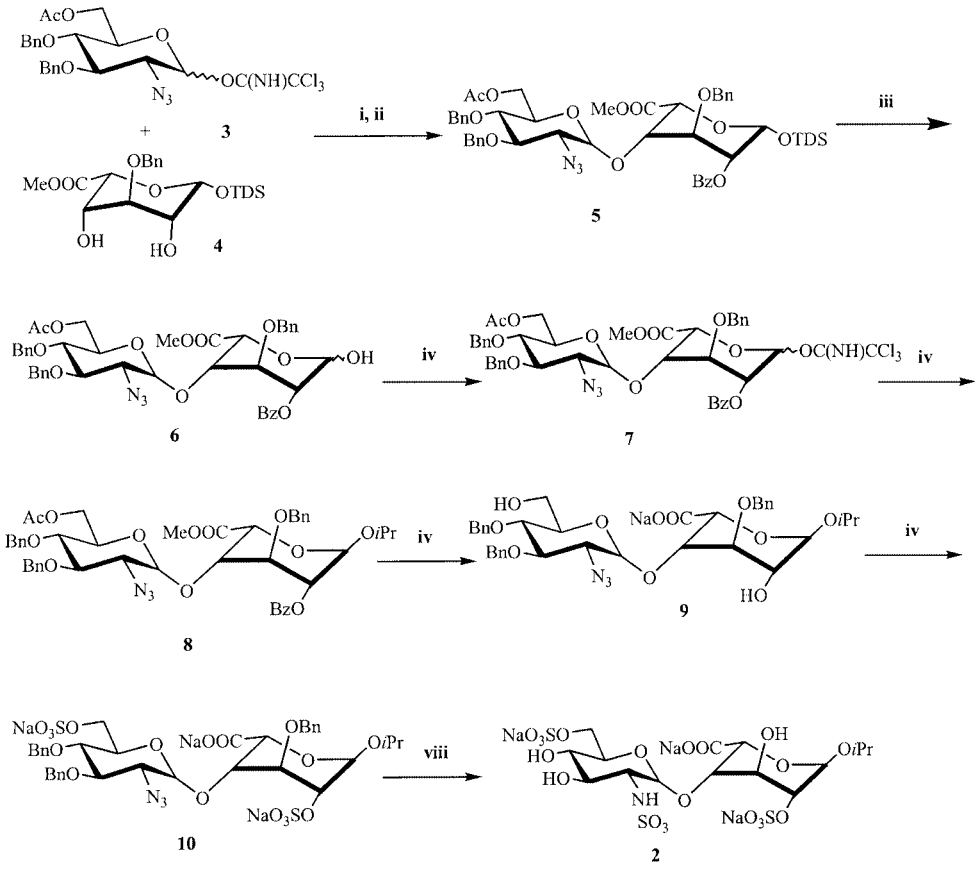

Scheme 1. Total synthesis of the disaccharide **2**: i) TMSOTf 3%, CH_2Cl_2, 0 °C; ii) BzCl, Py, 70% two steps; iii) $(HF)_n$·Py/THF, 5 °C, 85%; iv) CCl_3CN, K_2CO_3, CH_2Cl_2, 90%; v) *i*PrOH, TMSOTf, CH_2Cl_2, 60%; vi) a) LiOH 1 M, H_2O_2, THF; b) NaOH 4 N, MeOH, 89% two steps; vii) SO_3·Py, Py, 88%; viii) a) H_2, Pd/C, MeOH/H_2O, 9:1, 95%; b) SO_3·Py, H_2O pH = 9.5, 80%; TDS = dimethylthexysilyl chloride

Table 3. Most favourable interaction energies calculated for minimised **2** with all iduronate residues in the $^1C_4$ and ^2S_O conformations (in kcal·mol^{-1})

Metal cation	$^1C_4$	^2S_O
Ca^{2+}	−60	−51
Na^+	−33	−28
Mg^{2+}	−33	–

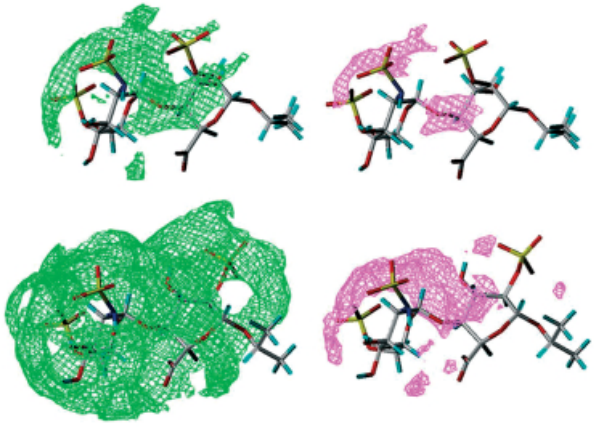

Figure 4. Structures of disaccharide **1** used for the calculation of the cation interaction energy and the volumes of the regions of the interaction potential within 15 kcal·mol^{-1} above the lowest value for calcium (right) and sodium (left) for $^1C_4$ (top) and ^2S_O (bottom)

The influence of Ca^{2+} on the structure of the disaccharide **2** was then investigated by NMR spectroscopy. Both chemical shifts and coupling constants of the iduronate ring were monitored in a Ca^{2+} acetate titration of the sodium salt of **2**. In order to determine whether the observed shifts were due to salt effects rather than to Ca^{2+}-specific effects, a parallel titration with sodium acetate was performed under the same conditions. Sodium acetate, even in excess (15 mol-equiv.), did not produce any change greater than experimental uncertainty either in chemical shifts or in coupling constants (Figure 5). Calcium acetate, in contrast, induced changes in both chemical shifts and coupling constants. Therefore, these changes should be attributed specifically to Ca^{2+} binding rather than to changes in the ionic strength. As these changes were small, their values were carefully calculated by full line-shape analysis of the spectra (Table 4 and Figure 5).

The chemical shifts observed in the spectrum of the sodium salt of **2** and those of the corresponding units (A and F units, Figure 1) in the sodium salt of **1** presented similar values. The differences between the chemical shifts of the

Table 4. ^{1}H chemical shifts for **1** and **2** as sodium salts and after addition of 12 mol-equiv. (for **1**) and 5 mol-equiv. (for **2**) of calcium in D_2O at 25 °C referenced to acetone; data for **1** are given for the three disaccharide units

	2 Na	**1** AB Na	**1** CD Na	**1** EF Na	**2** Ca	**1** AB Ca	**1** CD Ca	**1** EF Ca
IdoA H-1	5.26	5.26	5.28	5.22	5.30	5.38	5.48	5.39
IdoA H-2	4.19	4.18	4.34	4.33	4.20	4.24	4.42	4.39
IdoA H-3	4.21	4.20	4.21	4.20	4.22	4.24	4.31	4.28
IdoA H-4	4.04	4.04	4.09	4.10	4.05	4.07	4.12	4.14
IdoA H-5	4.54	4.54	4.86	4.83	4.57	4.63	4.98	4.92
GlcN H-1	5.33	5.34	5.41	5.44	5.32	5.32	5.37	5.43
GlcN H-2	3.24	3.27	3.27	3.23	3.25	3.30	3.32	3.29
GlcN H-3	3.67	3.70	3.66	3.63	3.68	3.83	3.78	3.68
GlcN H-4	3.57	3.79	3.78	3.56	3.58	3.88	3.88	3.62
GlcN H-5	3.96	4.00	4.03	3.99	3.96	4.06	4.10	4.02

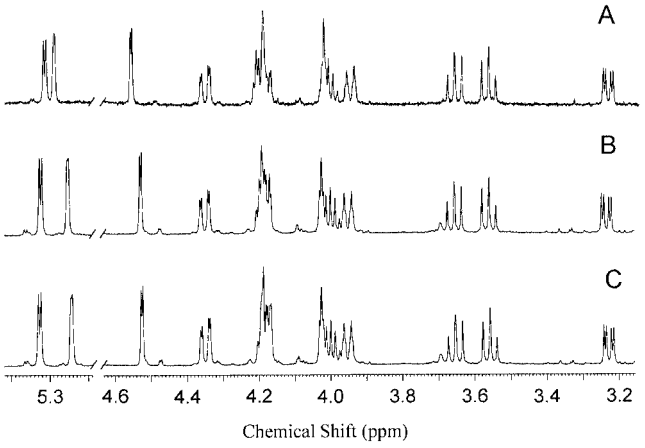

Figure 5. ^{1}H NMR spectra (D_2O, 25 °C, pH* = 7.4, 500 MHz) of: a) **2** in the presence of 5 mol-equiv. of calcium acetate; b) in the presence of 15 mol-equiv. of sodium acetate, and c) **2** sodium salt

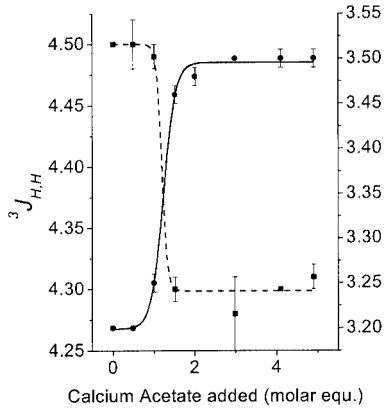

Figure 6. Variation of the significant $^3J_{H,H}$ coupling constants with addition of calcium in Hz; solid line and left scale: 2-H/3-H, and dashed line, right scale: 3-H/4-H

iduronate ring of **2** and those of unit A in **1** were smaller than 0.01 ppm. The values for the glucosamine ring of **2** and those of unit F in **1** were also almost identical, with the exception of H-1, which was closer to H-1 of unit B in the spectrum of **1**. The largest displacements on addition of Ca^{2+} were represented by H1 and H5 in the iduronate unit, which were shifted downfield (0.04 and 0.03 ppm, respectively). These were also the more perturbed protons in the case of **1**,[10] although the observed downfield shifts were larger (0.17−0.10 ppm for IdoA H1 and 0.09−0.07 for IdoA H5) for the hexasaccharide.[10] Also in common with the hexasaccharide, the signal of the anomeric proton of the glucosamine ring was shifted upfield. The chemical shift vs. Ca^{2+} concentration curves of **2** did not reach a plateau even at 5 mol-equiv. of salt, and so it was not possible to determine any binding constant. The behaviour of the coupling constants $J_{2,3}$ and $J_{3,4}$ for the iduronate unit upon calcium titration corresponded to a neat titration curve (Figure 6). This change in the coupling constant values, which had been reported previously,[1,14] was due to changes in the population balance of the two conformational forms of the iduronate ring towards the $^1C_4$ form.[14] The equivalence points for the curves were 1.2±0.7 and 1.23±0.03 Hz for $J_{H2\text{-}H3}$ and $J_{H3\text{-}H4}$, respectively. From these values a dissociation constant of 8.0 mM was calculated.

NOESY experiments were recorded both for the sodium salt and in the presence of 5 equiv. of Ca^{2+}, as well as at certain points of the Ca^{2+} or Na^+ titrations. Several mixing times were recorded and σ^{NOE} values for **2** sodium salt were calculated from the growth rates of normalized cross-peaks. These results were also similar to those found for the hexasaccharide **1**, with the obvious exception that no contribution of anisotropy was observed. This was due to the spherical molecular shape of **2**, in contrast to the top rotor form of **1**.[13] The changes observed in the presence of Ca^{2+} were mainly due to the displacement of the conformational equilibrium of the iduronate ring, a decrease being observed in the relative intensity of the NOE between the 2-H/5-H protons of this residue. The internal motion due to the iduronate conformational equilibrium precluded quantification of the distance of the NOE around the glycosidic linkage.

The ability of disaccharide **2** to interact with Ca^{2+} corroborated the main proposal for the binding site for hexasaccharide **1**.[10] The differences in affinity between **1** and **2** could be attributed to the lower total charge of the disacch-

aride. This was also manifested by the calculated interaction energy, which was more favourable for **1**.

Conclusion

Modelling techniques can provide valuable information on cation binding properties of GAGs, by combining dynamic information together with accurate evaluation of the interaction energy defining the most favourable binding regions. The combination of MD simulations with cation interaction potential calculations is able to reproduce some known features of heparin−cation interaction, such as the Ca^{2+} preference for the $^1C_4$ iduronate form[14] as well as the similarities between Na^+ and Mg^{2+} behaviour and their difference from that of Ca^{2+}.[9] The site-binding observed for Ca^{2+} might therefore reflect the existence of a specific binding site suitable for both Ca^{2+} size and charge, but not for Na^+ charge nor for Mg^{2+} size. This binding site is contained within the GlcN-IdoA disaccharide, in agreement with the previously proposed Ca^{2+} main binding site.[10]

The NMR study with **2** indicated that this model was able to bind Ca^{2+} and to reproduce some features of the heparin−Ca^{2+} complex, including the increase in the iduronate $^1C_4$ conformer population. It should be noted that the size of **2** prevented the occurrence of polyionic territorial binding.[8] However, the disaccharide interaction was weaker than that of the larger homologue **1**. This difference may be explained by the loss of medium- and long-range electrostatic interactions in the case of **2**, or by entropic contribution from a network of binding sites.[10]

The reported modelling and NMR results, together with the previous study of the hexasaccharide **1**, strongly suggest the presence of a Ca^{2+} binding site in heparin. The existence of this site might also be deduced from heparin deviations from Manning polyelectrolyte "two-variable" theory in the presence of Ca^{2+}.[8,9] According to our results, this site should be located between adjacent $GlcN_{i+1}$ and $IdoA_i$ residues corresponding to the optimum computed interaction energy regions. This site is able to match the Ca^{2+} coordinating shell through coordination of the COO^- and OSO_3^- groups of the iduronate residues and the $HNSO_3^-$ moiety in the glucosamine unit with the glycosidic and iduronate ring oxygen atoms and an apical water molecule. This square-bipyramid geometry involving an NH group and a water molecule has already been found in protein calcium complexes.[16] Finally, it should be stressed that these results do not contradict possible Ca^{2+} delocalisation among the binding sites through a charged groups network.[10]

Experimental Section

Computational Methods: The interaction energy surfaces were calculated by using GRID[11] and the corresponding cation as the probe.[12] The spacings between the calculated points were 0.33 Å, the dielectric constants used were 20 for the ligand and 80 for the water. Three enthalpic components were considered: Lennard−Jones potential, hydrogen bond, and electrostatic potential. The calculated surfaces were analysed by using SYBYL,[17] representing the volume above the best interaction energy. The structures used for calculation of the energy surface with the cations were constructed on the basis of previous MD results.[13] The values of significant torsion angles were taken from the MD by analysis of their distributions along the trajectory. Two subminima were considered for the two IdoA-GlcN glycosidic linkages, together with three rotamers for the sulfate groups, as well as the two iduronate conformers $^1C_4$ and ^2S_O. These values were introduced into a previously minimised structure and used without further modification. Seven of the 32 initially constructed structures were discarded due to high steric hindrance, and 25 rotamers were then considered. The structures used for comparison of the interaction energies with calcium, sodium, and magnesium were constructed by relaxation of the adequate conformer by AMBER[18] 5.0 with GLYCAM[19] carbohydrate parameters in the case of **1** without cations, or SYBYL[17] and PIM[20] parameters in the other cases, by 500 cycles of steepest descent followed by 5000 of conjugate gradients or until lower than $1\cdot10^{-4}$.

NMR Measurements: The disaccharide **2** (4.5 mg) was carefully desalted, and the counterion was completely exchanged for Na^+ with DOWEX-Na exchange resin and dissolved in D_2O (500 μL), with traces of acetone serving as internal reference (δ = 2.225 ppm). The ^1H NMR spectrum was assigned with the aid of COSY-dqf,[21] TOCSY,[22] and NOESY[23] experiments. The sample was titrated by addition of small aliquots from a solution of calcium acetate at pH* = 7.4 and the relative concentrations were checked by integration of the methyl signal of the acetate. The same procedure was used for the sodium acetate titration. The chemical shifts and coupling constants were calculated from full line-shape simulation of the collected ^1H spectra by gNMR.[24] NOESY experiments for the calculation of NOE cross relaxation rates were collected at several mixing times (100−500 ms), and the relaxation rates were calculated from the intensity of the NOE peaks growth rate.[25]

Synthesis

General Procedures: TLC analysis was performed on 60 F_{254} silica gel precoated on aluminium plates (Merck) and the compounds were detected by staining with sulfuric acid/ethanol (1:9, v/v) or with anisaldehyde solution (25 mL of anisaldehyde with 25 mL of sulfuric acid, 450 mL of ethanol, and 1 mL of acetic acid) followed by heating at 200 °C. Column chromatography was carried out on 60 silica gel (0.2−0.5 mm; 0.2−0.063 mm; 0.040−0.015 mm; Merck). Optical rotations were determined with a Perkin−Elmer 341 polarimeter. ^1H and ^{13}C NMR spectra were acquired with Bruker DPX 300, DRX 400, and DRX 500 spectrometers, and chemical shifts are given in ppm relative to TMS as indirect reference or relative to D_2O. Elemental analyses were performed with a Leco CHNS-932 apparatus, after drying of analytical samples over phosphorus pentoxide for 24 h. Gel filtration (Sephadex LH-20 and G-25; Pharmacia) and ion-exchange chromatography (Dowex 50WX4 Na^+; Fluka) were used to achieve the purification of the final products. MALDI-TOF mass spectra were recorded with a MALDI-TOF GSG System spectrometer.

Starting Materials: 6-*O*-Acetyl-2-azido-3,4-di-*O*-benzyl-2-deoxy-α,β-D-glucopyranosyl trichloroacetimidate (**3**)[26] and methyl (dimethylthexylsilyl 3-*O*-benzyl-β-L-idopyranosyl)uronate (**4**)[27,28] were prepared according to literature procedures.

Methyl [Dimethylthexylsilyl 4-*O*-(6-*O*-acetyl-2-azido-3,4-di-*O*-benzyl-2-deoxy-α-D-glucopyranosyl)-2-*O*-benzoyl-3-*O*-benzyl-β-L-idopyranosyl] Uronate (5): TMSOTf (39 μL, 0.216 mmol) was added under argon to a cooled (0 °C) solution of **3** (1.90 g, 4.32 mmol) in dry CH_2Cl_2 (100 mL). While the reaction mixture was stirred, a solution of **4** (2.48 g, 4.32 mmol) in dry CH_2Cl_2 (25 mL) was added dropwise. After 30 min, the mixture was neutralised with saturated $NaHCO_3$ solution, and CH_2Cl_2 (400 mL) was then added at room temp. The suspension was washed with H_2O (250 mL). The organic layer was dried with $MgSO_4$ and concentrated under vacuum, the residue was purified by flash chromatography (12:1, toluene/ethyl acetate) to obtain unchanged acceptor (363 mg, 19%), and the disaccharide was directly dissolved in Py (15 mL). Benzoyl chloride (4.1 mL, 35.21 mmol) was added, and the solution was stirred at room temp. After 24 h, the mixture was diluted with CH_2Cl_2 (400 mL), washed with H_2O (300 mL), dried with $MgSO_4$, and concentrated under vacuum. The residue was purified by flash chromatography [toluene/ethyl acetate (12:1)] to yield **5** (2.115 g, 51%). $[\alpha]_D^{r.t.} = +18.0$ ($c = 1$, $CHCl_3$); TLC [toluene/ethyl acetate (12:1)]: $R_f = 0.26$. ^1H NMR (500 MHz, $CDCl_3$): δ = 8.11−7.22 (m, 20 H, Ph), 5.17 (br. s, 1 H, H^1), 5.07 (br. s, 1 H, H^2), 4.84−4.74 (2 d, $J_{gem} = 11.7$ Hz, 2 H, CH_2Ph), 4.72 (d, $J_{1',2'} = 3.4$ Hz, 1 H, $H^{1'}$), 4.67−4.49 (2 d, $J_{gem} = 10.7$ Hz, 2 H, CH_2Ph), 4.48 (br. s, 1 H, H^5), 4.38 (dd, $J_{5',6'a} = 1.8$ Hz, $J_{6'a,6'b} = 12.4$ Hz, 1 H, $H^{6'a}$), 4.30 (dd, $J_{5',6'b} = 2.3$ Hz, 1 H, $H^{6'b}$), 4.23 (m, 1 H, H^3), 4.07 (m, 1 H, $H^{5'}$), 4.01 (br. s, 1 H, H^4), 3.96−3.87 (2d, $J_{gem} = 10.7$ Hz, 2 H, CH_2Ph), 3.75 (s, 3 H, $COOCH_3$), 3.53−3.43 (m, 2 H, $H^{3'}$, $H^{4'}$), 3.12 (dd, $J_{2,3} = 10.1$ Hz, 1 H, $H^{2'}$), 1.99 (s, 3 H, $OCOCH_3$), 1.56 [m, 1 H, C$H(CH_3)_2$], 0.79−0.75 [4 s, 12 H, $C(CH_3)_2$, $CH(CH_3)_2$], 0.25−0.13 [2 s, 6 H, $Si(CH_3)_2$] ppm. ^{13}C NMR (125 MHz, $CDCl_3$): δ = 170.6, 168.6, 166.5 (C=O), 137.8−127.7 (Ph), 99.6 ($C^{1'}$), 93.9 (C^1), 79.8, 77.3, 75.6, 75.0, 74.8, 74.6, 73.4, 73.0, 70.0, 68.7, 63.72, 62.29, 52.2 ($COOCH_3$), 33.9 [$CH(CH_3)_2$], 24.7 [$C(CH_3)_2$], 20.8 ($OCOCH_3$), 20.1−18.3 [$C(CH_3)_2$ and $CH(CH_3)_2$], −1.9, −3.3 [$Si(CH_3)_2$] ppm. MS-FAB: m/z = 976 [M + Na^+]. $C_{51}H_{63}N_3O_{13}Si$ (954.2): calcd. C 64.20, H 6.66, N 4.40; found C 64.47, H 6.64, N 4.24.

Methyl 4-*O*-(6-*O*-Acetyl-2-azido-3,4-di-*O*-benzyl-2-deoxy-α-D-glucopyranosyl)-2-*O*-benzoyl-3-*O*-benzyl-α,β-L-idopyranosuronate (6): An excess of $(HF)_n$·Py complex (3.1 mL) was added to a cooled (−10 °C) solution of **5** (1.067 g, 1.116 mmol) in dry THF (30 mL). The mixture was then allowed to warm to 0 °C and stirred under argon. After 24 h, CH_2Cl_2 (200 mL) was added, and the mixture was washed with H_2O (2 × 100 mL) and saturated $NaHCO_3$ solution (50 mL) until neutralisation. The organic layer was finally dried ($MgSO_4$) and concentrated in vacuo. Purification of the residue by flash chromatography [hexane/EA (2:1)] gave **5** (800 mg, 88%) as a α/β mixture. TLC [hexane/ethyl acetate (2:1)]: $R_f = 0.25$. ^1H NMR (500 MHz, $CDCl_3$): δ = 8.14−7.06 (m, 20 H, Ph), 5.45 (br. d, $J_{1\alpha,OH} = 8.4$ Hz, 0.5 H, $H^{1\alpha}$), 5.21 (br. d, $J_{1\beta,OH} = 9.0$ Hz, 0.5 H, $H^{1\beta}$), 5.06 (br. s, 1 H, H^2 α and β), 4.91 (br. s, 0.5 H, $H^{5\alpha}$), 4.91−4.85 (m, 1 H, CH_2Ph), 4.80−4.74 (2 d, J_{gem}= 11.5 Hz, J = 11.7 Hz, 1 H, CH_2Ph), 4.66−4.62 (m, 2 H, $H^{1'}$,CH_2Ph), 4.59 (br. s, 0.5 H, $H^{5\beta}$), 4.47 (m, 1 H, CH_2Ph), 4.37 (m, 1 H, $H^{6'a}$), 4.31 (m, 1 H, H^3), 4.25−4.19 (m, 1.5 H, $H^{6'b}$, OHα), 4.01−3.82 (m, 4 H, $H^{5'}$, H^4, CH_2Ph), 3.64 (m, 0.5 H, OHβ), 3.79 (s, 3 H, $COOCH_3$ α and β), 3.41 (m, 2 H, $H^{3'}$, $H^{4'}$), 3.19 (dd, $J_{1,2} = 3.7$ Hz, $J_{2,3} = 9.2$ Hz, 1 H, $H^{2'}$), 2.00 (s, 3 H, $OCOCH_3$ α and β) ppm. MS-FAB: m/z = 834 [M + Na^+]. $C_{43}H_{45}N_3O_{13}$ (811.8): calcd. C 63.62, H 5.59, N 5.18; found C 63.22, H 5.95, N 4.94.

***O*-[Methyl 4-*O*-(6-*O*-acetyl-2-azido-3,4-di-*O*-benzyl-2-deoxy-α-D-glucopyranosyl)-2-*O*-benzoyl-3-*O*-benzyl-α,β-L-idopyranosyluronate] Trichloroacetimidate (7):**[13] Cl_3CCN (593 μL, 5.90 mmol) and K_2CO_3 (55 mg, 0.39 mmol) were added to a solution of **6** (320 mg, 0.39 mmol) in dry CH_2Cl_2 (4 mL). After stirring at room temp. for 4 h, the mixture was filtered off and concentrated in vacuo, and the residue was purified on a short silica gel column [hexane/ethyl acetate (2:1)] to yield **6** (357 mg, 95%) as an α/β mixture. TLC [hexane/ethyl acetate (2:1)]: R_f = 0.53 and 0.38 (β and α). ^1H NMR (500 MHz, $CDCl_3$): δ = 8.67 (s, 0.6 H, NHβ), 8.64 (s, 0.4 H, NHα), 8.13−7.10 (m, 20 H, Ph), 6.55 (br. s, 0.6 H, $H^{1\beta}$), 6.29 (d, 0.4 H, $J_{1,2} = 1.8$ Hz, $H^{1\alpha}$), 5.43 (m, 0.4 H, $H^{2\alpha}$), 5.33 (br. s, 0.6 H, $H^{2\beta}$), 5.00 (br. s, 0.4 H, $H^{5\alpha}$), 4.93−4.88 (m, 1 H, 1× CH_2Ph), 4.79−4.65 (m, 3.6 H, $H^{5\beta}$, $H^{1'}$, 1× CH_2Ph), 4.52−4.46 (m, 1 H, 1× CH_2Ph), 4.38−4.35 (m, 1.4 H, $H^{6'a}$, $H^{3\alpha}$), 4.25−4.23 (m, 1.6 H, $H^{6'b}$, $H^{3\beta}$), 4.15 (br. s, 0.4 H, $H^{4\alpha}$), 4.03−3.88 (m, 3.6 H, $H^{5'}$, $H^{4\beta}$, CH_2Ph), 3.79−3.78 (2 s, 3 H, $COOCH_3$ α and β), 3.51−3.41 (m, 2 H, $H^{3'}$, $H^{4'}$), 3.23−3.19 (m, 1 H, $H^{2'}$), 1.99 (s, 3 H, $OCOCH_3$ α and β) ppm. $C_{45}H_{45}Cl_3N_4O_{13}$ (956.2): calcd. C 56.52, H 4.74, N 5.86; found C 56.17, H 4.98, N 5.79.

Methyl [Isopropyl 4-*O*-(6-*O*-acetyl-2-azido-3,4-di-*O*-benzyl-2-deoxy-α-D-glucopyranosyl)-2-*O*-benzoyl-3-*O*-benzyl-α-L-idopyranosyl] Uronate (8): Isopropyl alcohol (46 μL, 0.75 mmol) and TMSOTf (50 μL of a 0.18 M solution in dry CH_2Cl_2) were added under argon to a cooled (0 °C) solution of **7** (242 mg, 0.25 mmol) in dry CH_2Cl_2 (3 mL). After 5 min, the mixture was neutralised with saturated $NaHCO_3$ solution and diluted with CH_2Cl_2 (100 mL). The suspension was washed with H_2O (100 mL), and the organic layer was dried ($MgSO_4$) and concentrated in vacuo. The residue was purified by flash chromatography [hexane/ethyl acetate (6:1)] to yield the α anomer **7** (140 mg, 65%) and the β anomer (50 mg, 23%): $[\alpha]_D^{r.t.} = +22.5$ ($c = 1.1$, $CHCl_3$). TLC [hexane/EA (3:1)]: $R_f = 0.37$. ^1H NMR (500 MHz, $CDCl_3$): δ = 8.25−7.20 (m, 20 H, Ph), 5.28 (s, 1 H, H^1), 5.12(s, 1 H, H^2), 4.97 (d, 1 H, 1× CH_2Ph), 4.89 (d, $J_{5,4} = 2.5$ Hz, 1 H, H^5), 4.77 (d, $J_{1',2'} = 3.5$ Hz, 1 H, $H^{1'}$), 4.72 (m, 2 H, CH_2Ph), 4.37 (d, 1 H, 1× CH_2Ph), 4.36 (dd, $J_{5',6'a} = 2$ Hz, $J_{6'a,6'b} = 12.5$ Hz, 1 H, $H^{6'a}$), 4.26 (dd, $J_{5',6'a} = 3$ Hz, $J_{6'a,6'b} = 12.0$ Hz, 1 H, $H^{6'b}$), 4.14 (t, $J_{3,2} = J_{3,4} = 2.5$ Hz, 1 H, H^3), 4.09 (m, 2 H, H^4, 1× CH_2Ph), 4.00 [m, 3 H, 1× CH_2Ph, $H^{5'}$, C$H(CH_3)_2$], 3.77 (s, 3 H, $COOCH_3$), 3.55 (t, 1 H, $H^{3'}$), 3.45 (t, $J_{4',3'} = J_{4',5'} = 10$ Hz, 1 H, $H^{4'}$), 3.19 (dd, $J_{2',3'} = 3.5$ Hz, $J_{2,3} = 10.0$ Hz, 1 H, $H^{2'}$), 2.05(s, 3 H, $OCOCH_3$), 1.25−1.15 [m, 6 H, $CH(CH_3)_2$] ppm. ^{13}C NMR (125 MHz, $CDCl_3$): δ = 170.63, 169.90, 165.61 (C=O), 137.00−127.0 (Ph), 99.62 (C^1), 97.29 ($C^{1'}$), 80.15 ($C^{3'}$), 76.36 ($C^{4'}$), 74.86, 74.74 (CH_2Ph), 73.38 (C^4), 72.16 (C^3), 70.48 (C^5), 70.08 (CH_2Ph), 68.27(C^2), 67.46 ($C^{5'}$), 63.73 ($C^{6'}$), 62.38 ($C^{2'}$), 52.39 ($COOCH_3$), 23.35 ($OCOCH_3$) 21.47, 20.91 [$CH(CH_3)_2$] ppm. MALDI-TOF MS: m/z = 876 [M + Na^+], 892 [M + K^+]. $C_{46}H_{51}N_3O_{13}$ (853.9): calcd. C 64.77, H 5.97, N 4.92; found C 64.06, H 6.12; N 5.04.

Isopropyl 4-*O*-(2-Azido-3,4-di-*O*-benzyl-2-deoxy-α-D-glucopyranosyl)-3-*O*-benzyl-α-L-idopyranosiduronic Acid Sodium Salt (9): A solution of **8** (84 mg, 0.09 mmol) in THF (9.2 mL) was treated at 0 °C with hydrogen peroxide (30 wt% solution in water, 1.8 mL) and LiOH (1.0 M, 2.35 mL), and the mixture was stirred for 6 h at room temp. and was then cooled to 0 °C. MeOH (7.0 mL) and NaOH (4 N, 2.35 mL) were then added, and the mixture was stirred for 16 h and was treated with Amberlite IR-120 (H^+) resin until neutralisation, filtered, and concentrated under reduced pressure. The residue was eluted through Sephadex LH-20 chromatography column with CH_2Cl_2/MeOH (1:1) to afford **8** (60.4 mg, 89%). $[\alpha]_D^{r.t.} = -0.6$ ($c = 0.5$, MeOH). TLC [CH_2Cl_2/MeOH (10:1)]: R_f = 0.46. ^1H NMR (500 MHz, [D_4]methanol): δ = 7.38−7.12 (m, 15 H, Ph), 5.30 (s, 1 H, H^1), 5.03(s, 1 H, $H^{1'}$), 1.12 [m, 6 H,

$CH(CH_3)_2$]. MALDI-TOF MS: *m/z* = 716 [M + Na^+], 732 [M + K^+]. $C_{36}H_{43}N_3O_{11}$ (693.7): calcd. C 62.33, H 6.20, N 6.06; found C 61.93, H 6.38, N 6.17.

Isopropyl-*O*-(2-azido-3,4-di-*O*-benzyl-2-deoxy-6-*O*-sulfo-α-D-glucopyranosyl)-3-*O*-benzyl-2-*O*-sulfo-α-L-idopyranosiduronic Acid) Trisodium Salt (10): A mixture of **9** (53 mg, 0.07 mmol) and SO_3·Py complex (121.6 mg, 0.76 mmol) in dry Py (2 mL) was stirred under argon. After 1 h, the mixture was cooled and MeOH (2 mL) and CH_2Cl_2 (1 mL) were added. The solution was eluted through Sephadex LH-20 with CH_2Cl_2/MeOH (1:1). Fractions containing the disaccharide were concentrated and passed through Dowex 50WX4-Na^+ with MeOH/H_2O (2:1), to yield **10** (56.8 mg, 82%). $[\alpha]_D^{rt.}$ = −4.2 (*c* = 0.57, MeOH). TLC [EtOAc/Py/H_2O/AcOH (15:5:3:1)]: R_f = 0.5. ^{1}H NMR (500 MHz, [D_4]methanol): δ = 7.42−7.20 (m, 15 H, Ph), 5.26 (s, 1 H, H^1), 5.08 (d, $J_{1',2'}$ = 3.5 Hz, 1 H, $H^{1'}$), 4.80 (d, $J_{5,4}$ = 2.5 Hz, 1 H, H^5), 4.78 (m, 4 H, 2 CH_2Ph), 4.62 (d, 1 H, 1× CH_2Ph), 4.43 (s, 1 H, H^2), 4.31 (dd, $J_{5',6'a}$ = 2.5 Hz, $J_{6'a,6'b}$ = 10.5 Hz, 1 H, $H^{6'a}$), 4.14 (t, 1 H, H^3), 4.18 (dd, $J_{5',6'a}$ = 0.5 Hz, $J_{6'a,6'b}$ = 9 Hz, 1 H, $H^{6'b}$), 4.08 (s, 1 H, H^4), 3.92 [m, 1 H, $CH(CH_3)_2$], 3.87 (m, 2 H, $H^{3'}$, $H^{5'}$), 3.64 (t, $J_{4',3'}$ = $J_{4',5'}$ = 9.5 Hz, 1 H, $H^{4'}$), 3.41 (dd, $J_{2',3'}$ = 3.5 Hz, $J_{2,3}$ = 10.0 Hz, 1 H, $H^{2'}$), 1.24−1.19 [m, 6 H, $CH(CH_3)_2$] ppm. ^{13}C NMR (125 MHz, [D_4]methanol): δ = 172.5 (C=O), 138.00−127.2 (Ph), 97.63 (C^1), 95.31 ($C^{1'}$), 80.24 ($C^{3'}$), 77.60 ($C^{4'}$), 74.84 (CH_2Ph), 74.55 (C^5), 71.46 (CH_2Ph), 70.85 (C^2, C^3, C^4), 70.26 [$C^{5'}$, $CH(CH_3)_2$], 65.57 ($C^{6'}$), 63.76 ($C^{2'}$), 22.23, 20.53 [$CH(CH_3)_2$] ppm. MALDI-TOF MS: *m/z* = 941.7 [M + Na^+], 957.8 [M + K^+]. $C_{36}H_{40}N_3Na_3O_{17}S_2$ (919.8): calcd. C 47.0, H 4.35, N 4.57; found C 47.2, H 4.72, N 4.31.

Isopropyl-*O*-(2-deoxy-2-sulfamino-6-*O*-sulfo-α-D-glucopyranosyl)-2-*O*-sulfo-α-L-idopyranosiduronic Acid) Tetrasodium Salt (2): A solution of **10** (47 mg, 0.05 mmol) in MeOH/H_2O (9:1; 1.5 mL) was hydrogenated in the presence of 10% Pd/C. After 24 h, the suspension was filtered and concentrated to give the desired product, which was homogeneous by TLC analysis with EtOAc/Py/H_2O/AcOH (8:5:3:1) as eluent (R_f = 0.26). No aromatic signal was detected by NMR spectroscopy. This compound was directly used for the *N*-sulfation. The hydrogenated disaccharide {TLC [EtOAc/Py/H_2O/AcOH (6:5:3:1)]: R_f = 0.6; ^{1}H NMR (500 MHz, D_2O): δ = 5.17 (d, 1 H, $H^{1'}$), 5.12 (s, 1 H, H^1), 4.55 (s, 1 H, H^2), 4.28 (d, 1 H, $H^{6'a}$), 4.18 (s, 1 H, H^4), 4.11 (m, 2 H, $H^{6'b}$, H^5), 4.01 (s, 1 H, H^3), 3.94 [m, 1 H, $CH(CH_3)_2$], 3.86 (d, $J_{5',4'}$ = 9 Hz, 1 H, $H^{5'}$), 3.65 (t, $J_{3',2'}$ = $J_{3',4'}$ = 9.5 Hz, 1 H, $H^{3'}$), 3.45 (t, $J_{4',5'}$ = $J_{4',3}$ = 9.5 Hz, 1 H, $H^{4'}$), 2.92 (dd, 1 H, $H^{2'}$), 1.13 [m, 6 H, $CH(CH_3)_2$] ppm; ^{13}C NMR (125 MHz, [D_4]methanol): δ = 173.1 (C=O), 96.2 ($C^{1'}$), 93.8 (C^1), 72.9 (C^5), 71.1 ($C^{3'}$), 71.0 [$CH(CH_3)_2$], 70.9 (C^3), 69.7($C^{5'}$), 68.3 ($C^{4'}$), 65.9 (C^2), 65.8 ($C^{6'}$), 63.3 (C^4), 54.1 ($C^{2'}$), 21.8, 20.2 [$CH(CH_3)_2$]} was dissolved in H_2O (1 mL) and the pH of the solution was adjusted to 9.5 with NaOH solution (1 N). SO_3·Py complex (30 mg, 5 equiv.) was added in three portions over 1 h and the pH was maintained at 9.5 by subsequent addition of 1 N NaOH solution. A fourth, fifth, and sixth portion of pyridine−sulfur trioxide complex were added after 2, 4, and 6 h of stirring, respectively. After 24 h, the mixture was neutralised to pH = 7 with 0.1 N HCl solution and then chromatographed on a column of Sephadex G-25 with 0.9% NaCl solution. The appropriate fractions were pooled and passed through a Dowex 50WX4-Na^+ column with 0.5 M NaCl solution and then a Sephadex G-25 column with H_2O/EtOH (9:1). The fractions, which contained the final disaccharide **2**, were lyophilised to give (23 mg, 80%). Before NMR studies, it was useful to perform a final elution on a Dowex 50WX4-Na^+ column in order to avoid the formation of calcium salts instead of sodium salts and to obtain better resolution in the spectra. **Disaccharide 2:** TLC [EtOAc/Py/H_2O/AcOH (4:5:3:1)]: R_f = 0.55. ^{1}H NMR (500 MHz, D_2O): δ = 5.15 (m, 2 H, $H^{1'}$,H^1), 4.60 (s, 1 H, H^5), 4.16 (m, 2 H, $H^{6'}$, H^3), 4.03 (m, 2 H, H^2, $H^{6'b}$), 3.89 (s, 1 H, H^4), 3.83 [m, 1 H, $CH(CH_3)_2$], 3.68 (d, $J_{5',4'}$ = 9.5 Hz, 1 H, $H^{5'}$), 3.46 (t, $J_{3',2'}$ = $J_{3',4'}$ = 10 Hz, 1 H, $H^{3'}$), 3.40 (t, $J_{4',5'}$ = $J_{4',3'}$ = 10 Hz, 1 H, $H^{4'}$), 3.06 (dd, $J_{2',1'}$ = 3 Hz, $J_{2',3'}$ = 10.0 Hz, 1 H, $H^{2'}$), 1.02 [m, 6 H, $CH(CH_3)_2$] ppm. ^{13}C NMR (125 MHz, [D_4]methanol): δ = 168.1 (C=O), 98.2 ($C^{1'}$), 97.1 (C^1), 76.2 (C^5), 74.0 ($C^{3'}$), 71.5 [$CH(CH_3)_2$], 70.0 (C^3), 69.9($C^{5'}$), 68.6 ($C^{4'}$), 66.3 (C^2), 65.9 ($C^{6'}$,C^4), 57.5 ($C^{2'}$), 21.8, 20.2 [$CH(CH_3)_2$]. MALDI-TOF MS: *m/z* = 748.2 [M + Na^+], 764.8 [M + K^+].

Acknowledgments

Thanks are given to the DGSE (Grant PB96 0820) for financial support. F. C. and J. A. are grateful for predoctoral fellowships to the European Union (TMR Programme: GLYCOTRAIN) and the Fundación Ramón Areces, respectively. We thank Dr. Ezequiel Quintana for his technical help with GRID software.

[1] B. Casu, *Adv. Carbohydr. Chem. Biochem.* **1985**, *43*, 51−134.
[2] K. Salminista, K. Lidtholt, U. Lindahl, *FASEB J.* **1996**, *10*, 1270−1279.
[3] U. Lindahl, *Glycoconjugate J.* **2001**, *17*, 597−605.
[4] B. Mulloy, R. J. Linhardt, *Curr. Opin. Struct. Biol.* **2001**, *11*, 623−628.
[5] S. Faham, D. C. Rees, R. J. Linhardt, *Curr. Opin. Struct. Biol.* **1998**, *8*, 578−586.
[6] M. Kan, F. Wang, F. Xu, J. W. Craab, J. Hon, W. L. McKeehan, *Science* **1993**, *259*, 1918−1921.
[7] I. Capila, M. J. Hernaiz, Y. D. Mo, T. R. Mealy, B. Campos, J. R. Dedman, R. J. Linhardt, *Structure* **2001**, *9*, 57−64.
[8] G. S. Manning, *Acc. Chem. Res.* **1979**, *12*, 443−449.
[9] D. L. Rabenstein, J. M. Robert, J. Peng, *Carbohydr. Res.* **1995**, *218*, 239−256.
[10] J. Angulo, J. L. de Paz, P. M. Nieto, M. Martin-Lomas, *Isr. J. Chem.* **2000**, *40*, 289−299.
[11] P. S. Goodford, *J. Med. Chem.* **1985**, *28*, 849−857.
[12] I. Braccini, R. P. Grasso, S. Perez, *Carbohydr. Res.* **1999**, *317*, 119−130.
[13] J. L de Paz, J. Angulo, J-M. Lassaletta, P. M. Nieto, M. Redondo-Horcajo, R. M. Lozano, G. Giménez-Gallego, M. Martín-Lomas, *ChemBioChem* **2001**, *2*, 673−685.
[14] D Ferro, A. Provasoli, M. Ragazzi, B. Casu, G. Torri, V. Bossennec, B. Perly, P. Sinay, M. Petitou, J. Choay, *Carbohydr. Res.* **1990**, *195*, 157−167.
[15] B. Mulloy, M. Foster, *Glycobiology* **2000**, *10*, 1147−1156.
[16] A. K. Katz, J. P. Glusker, S. A. Beebe, C. W. Bock, *J. Am. Chem. Soc.* **1996**, *118*, 5752−5763.
[17] SYBYL® 6.7.1, Tripos Inc., 1699 South Harley Rd., St. Louis, Missouri, 63144, USA.
[18] D. A. Case, D. A. Pearlman, J. W. Caldwell, T. E. Cheatham III, W. S. Ross, C. L. Simmerling, T. A. Darden, K. M. Merz, R. V. Stanton, A. L. Cheng, J. J. Vincent, M. Crowley, D. M. Ferguson, R. J. Radmer, G. L. Seibel, U. C. Singh, P. K. Weiner, P. A. Kollman, *AMBER 5*, University of California, San Francisco, **1997**.
[19] R. J. Woods, R. A. Dwek, C. J. Edge, B. Fraiser-Reid, *J. Phys. Chem.* **1995**, *99*, 3832−3846.
[20] S. Perez, C. Meyer, A. Imberty, *Modelling of Biomolecular Structures and Mechanisms* (Eds.: A. Pullman, J. Jortner, B. Pullman), Kluwer Academic Press, Dordrecht, **1995**, pp. 425−444.
[21] A. L. Davis, E. D. Lane, J. Keeler, D. Moskau, J. Lohman, *J. Magn. Reson.* **1991**, *94*, 637−644.

[22] A. Bax, D. G. Davis, *J. Magn. Reson.* **1985**, *65*, 355−360.
[23] J. Jeener, B. H. Meier, P. Bachmann, R. R. Ernst, *J. Chem. Phys.* **1983**, *71*, 4546−4553.
[24] GNMR© V4.1.0, The Magdalen Centre, Oxford Science Park, Oxford OX4 4GA, UK.
[25] D. Neuhaus, M. Williamson, *The Nuclear Overhauser Effect in Structural and Conformational Analysis*, VCH, New York, **1989**.
[26] D. Tailler, J. C. Jacquinet, A. M. Noirot, J. M. Beau, *J. Chem. Soc., Perkin Trans. 1* **1992**, 3163−3164.
[27] R. Ojeda, J. L. de Paz, M. Martín-Lomas, J. M. Lassaletta, *Synlett* **1999**, *8*, 1316−1318.
[28] A. Lubineau, O. Gavard, J. Alais, D. Bonnaffé, *Tetrahedron Lett.* **2000**, *41*, 307−311.

Received January 15, 2002
[O02016]